

Stimulation of the cardiopulmonary baroreflex enhances ventricular contractility in awake dogs: a mathematical analysis study

Javier A. Sala-Mercado,^{1*} Mohsen Moslehpour,^{2*} Robert L. Hammond,¹ Masashi Ichinose,¹ Xiaoxiao Chen,² Sell Evan,¹ Donal S. O'Leary,¹ and Ramakrishna Mukkamala²

¹Department of Physiology and Cardiovascular Research Institute, Wayne State University School of Medicine, Detroit, Michigan; and ²Department of Electrical and Computer Engineering, Michigan State University, East Lansing, Michigan

Submitted 15 November 2013; accepted in final form 17 June 2014

Sala-Mercado JA, Moslehpour M, Hammond RL, Ichinose M, Chen X, Evan S, O'Leary DS, Mukkamala R. Stimulation of the cardiopulmonary baroreflex enhances ventricular contractility in awake dogs: a mathematical analysis study. *Am J Physiol Regul Integr Comp Physiol* 307: R455–R464, 2014. First published June 18, 2014; doi:10.1152/ajpregu.00510.2013.—The cardiopulmonary baroreflex responds to an increase in central venous pressure (CVP) by decreasing total peripheral resistance and increasing heart rate (HR) in dogs. However, the direction of ventricular contractility change is not well understood. The aim was to elucidate the cardiopulmonary baroreflex control of ventricular contractility during normal physiological conditions via a mathematical analysis. Spontaneous beat-to-beat fluctuations in maximal ventricular elastance (E_{\max}), which is perhaps the best available index of ventricular contractility, CVP, arterial blood pressure (ABP), and HR were measured from awake dogs at rest before and after β -adrenergic receptor blockade. An autoregressive exogenous input model was employed to jointly identify the three causal transfer functions relating beat-to-beat fluctuations in CVP to E_{\max} ($\text{CVP} \rightarrow E_{\max}$), which characterizes the cardiopulmonary baroreflex control of ventricular contractility, ABP to E_{\max} , which characterizes the arterial baroreflex control of ventricular contractility, and HR to E_{\max} , which characterizes the force-frequency relation. The $\text{CVP} \rightarrow E_{\max}$ transfer function showed a static gain of $0.037 \pm 0.010 \text{ ml}^{-1}$ (different from zero; $P < 0.05$) and an overall time constant of $3.2 \pm 1.2 \text{ s}$. Hence, E_{\max} would increase and reach steady state in $\sim 16 \text{ s}$ in response to a step increase in CVP, without any change to ABP or HR, due to the cardiopulmonary baroreflex. Following β -adrenergic receptor blockade, the $\text{CVP} \rightarrow E_{\max}$ transfer function showed a static gain of $0.0007 \pm 0.0113 \text{ ml}^{-1}$ (different from control; $P < 0.10$). Hence, E_{\max} would change little in steady state in response to a step increase in CVP. Stimulation of the cardiopulmonary baroreflex increases ventricular contractility through β -adrenergic receptor system mediation.

beat-to-beat variability; cardiopulmonary baroreflex; maximal ventricular elastance; system identification; ventricular contractility

THE BAROREFLEX SYSTEMS ARE primarily responsible for maintaining blood pressure in the short term (seconds to minutes) and also appear to contribute to longer-term blood pressure regulation (29, 30). It is well known that the arterial baroreflex senses arterial blood pressure (ABP) via stretch receptors lying in the carotid sinus and aortic arch and buffers an increase in ABP by decreasing, for example, total peripheral resistance (TPR), heart rate (HR), and ventricular contractility. The sensory receptors of the cardiopulmonary baroreflex are more

complex, residing mainly in the cardiac chambers but also in the pulmonary vessels (5). These receptors have been shown to be responsive to both central venous pressure (CVP) (7, 25) and left atrial pressure (LAP) (10, 21), which often change in parallel. The cardiopulmonary baroreflex responds to a change in these pressures by inducing an opposite change in TPR (1, 16, 25). An increase in the preload pressures also leads to an increase in HR (i.e., Bainbridge effect) in dogs (3), but an opposite change may occur in humans (7).

However, the cardiopulmonary baroreflex control of ventricular contractility is not well understood. Teleologically, a change in CVP/LAP could induce a same directional change in ventricular contractility so as to maintain central blood volume, much like the Bainbridge effect. On the other hand, a change in these pressures could cause an opposite direction change in ventricular contractility to blunt the forthcoming change in ABP due to the altered preload, much like the cardiopulmonary baroreflex control of TPR. Experimentally, previous studies have produced conflicting results. Ramchandra et al. (24) showed that cardiac sympathetic nerve activity changes in the opposite direction of CVP in conscious sheep during blood volume changes. By contrast, Karim et al. (10) demonstrated that cardiac sympathetic nerve activity increases, while renal sympathetic nerve activity decreases, in response to stimulation of the cardiopulmonary baroreflex via left atrial balloon distension in anesthetized dogs. Furnival et al. (9) reported that the maximal derivative of left ventricular pressure (LVP) does not significantly change following left atrial balloon distension in anesthetized dogs. By contrast, Kurz et al. (12) showed that the maximal LVP derivative (adjusted by LVP to compensate for preload) increased using a similar preparation with some or none of the potential confounding mechanisms (e.g., carotid sinus baroreflex) blocked. Factors that could have contributed to these contrasting results include use of different and limited (e.g., load-dependent) ventricular contractility indices, potential confounding mechanisms that were left totally or partially intact, and variations between conscious and anesthetized states.

In this study, our aim was to elucidate the cardiopulmonary baroreflex control of ventricular contractility during normal physiological conditions via analysis of spontaneous beat-to-beat fluctuations in multiple hemodynamic variables from awake dogs before and after β -adrenergic receptor blockade. We measured left ventricular maximal elastance (E_{\max}), which is generally considered the best, scalar index of ventricular contractility, and identified the transfer function relating beat-to-beat fluctuations in CVP to E_{\max} , while mathematically eliminating potential confounding mechanisms, including the arterial baroreflex. Our major finding is that the cardiopulmo-

* J. A. Sala-Mercado and M. Moslehpour contributed equally to this article.

Address for reprint requests and other correspondence: R. Mukkamala, Dept. of Electrical and Computer Engineering, Michigan State Univ., 428 S. Shaw Lane, Rm. 2120 Engineering Bldg., East Lansing, MI 48824-1226 (e-mail: rama@egr.msu.edu).

nary baroreflex responds to an increase in CVP by increasing ventricular contractility in awake dogs. A pilot version of this study has been reported in an abbreviated form (27).

MATERIALS AND METHODS

Overview and Rationale of Mathematical Analysis

The idea is to quantitatively characterize the cardiopulmonary baroreflex control of ventricular contractility by applying system identification to beat-to-beat hemodynamic variability, occurring naturally at rest. Since CVP and LAP may be positively correlated under these circumstances, CVP is arbitrarily selected as the input to this system. E_{max} is chosen as the output, because it may be more sensitive and specific to ventricular contractility than other available indices. The system is considered to be linear and time-invariant, as hemodynamic fluctuations at rest are often small and relatively stationary (32). Hence, the transfer function relating beat-to-beat fluctuations in CVP to E_{max} ($\text{CVP} \rightarrow E_{\text{max}}$) is specifically sought for identification. The identified transfer function will not only indicate whether E_{max} increases or decreases in the steady state in response to a step increase in CVP (static behavior) but also the time course that E_{max} takes in reaching the steady-state level (dynamic behavior).

However, as suggested in Fig. 1, identification of the $\text{CVP} \rightarrow E_{\text{max}}$ transfer function may be confounded by other physiological mechanisms. That is, an increase in CVP will cause an increase in HR (in dogs via the Bainbridge effect). This increase will, in turn, cause E_{max} to increase via the force-frequency relation. So, in this case, an increase in CVP will cause E_{max} to increase. But, the mechanism here is not the cardiopulmonary baroreflex. An increase in CVP will also cause an increase in ABP via preload enhancement. This increase will cause E_{max} to decrease via the arterial baroreflex. So, in this case, an increase in CVP will cause E_{max} to decrease. But, again, this mechanism is not the cardiopulmonary baroreflex. To determine the direct effects of fluctuations of CVP on E_{max} , the transfer function relating fluctuations in ABP to E_{max} ($\text{ABP} \rightarrow E_{\text{max}}$), which characterizes the arterial baroreflex control of E_{max} , and the transfer function relating fluctuations in HR to E_{max} ($\text{HR} \rightarrow E_{\text{max}}$), which characterizes the force-frequency relation, are simultaneously identified with the $\text{CVP} \rightarrow E_{\text{max}}$ transfer function (dark lines and font in Fig. 1). Further, as indicated in Fig. 1, the resultant change in E_{max} may alter both CVP and ABP via a change in the cardiac output curve of the heart-lung unit. In other words, the inputs and output may be related in closed-loop with CVP, ABP, and HR fluctuations causing E_{max} fluctuations (feed-back pathway, gray lines and fonts in Fig. 1) and E_{max} fluctuations, in turn, causing CVP and ABP fluctuations (feed-forward pathway).

loop systems as they operate in closed-loop, the identification is based on a parametric model so that causality can be enforced (31).

Since spontaneous hemodynamic variability contains limited information, the following parsimonious autoregressive exogenous input (ARX) model is specifically employed:

$$E_{\text{max}}(t) = \sum_{i=1}^p a_i \cdot E_{\text{max}}(t-i) + \sum_{i=0}^n b_i \cdot \text{HR}(t-i) + \sum_{i=s}^m c_i \cdot \text{ABP}(t-i) + \sum_{i=q}^r d_i \cdot \text{CVP}(t-i) + W_{E_{\text{max}}}(t) \quad (1)$$

where t is discrete time (15). The four sets of unknown parameters $\{a_i, b_i, c_i, d_i\}$ fully define the three transfer functions as follows:

$$\text{HR} \rightarrow E_{\text{max}} : \frac{\sum_{k=0}^n b_k e^{-j\omega k}}{1 - \sum_{k=1}^p a_k e^{-j\omega k}} \quad (2)$$

$$\text{ABP} \rightarrow E_{\text{max}} : \frac{\sum_{k=s}^m c_k e^{-j\omega k}}{1 - \sum_{k=1}^p a_k e^{-j\omega k}} \quad (3)$$

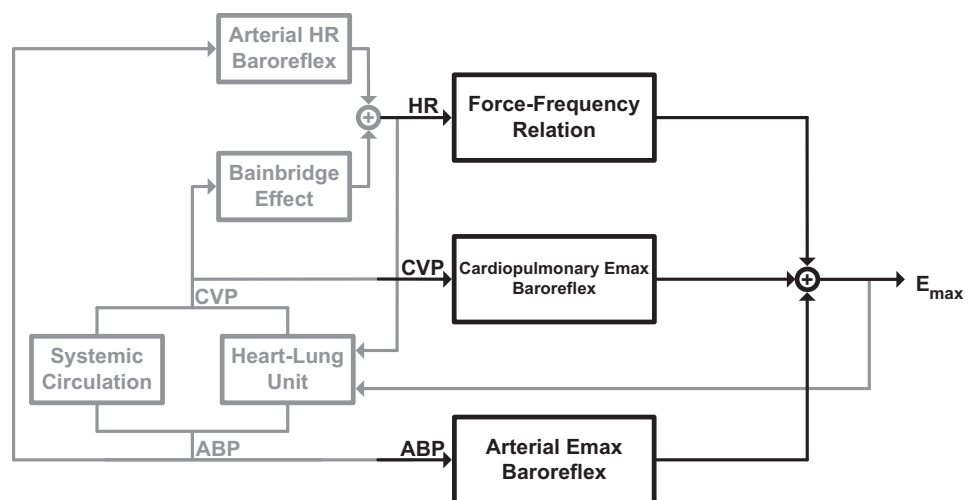
$$\text{CVP} \rightarrow E_{\text{max}} : \frac{\sum_{k=q}^r d_k e^{-j\omega k}}{1 - \sum_{k=1}^p a_k e^{-j\omega k}} \quad (4)$$

where ω is frequency. The unmeasured residual error $W_{E_{\text{max}}}$ is defined as an uncorrelated, white noise process. This process and the set of unknown AR parameters $\{a_i\}$ together specify the component of E_{max} not due to the three inputs. This E_{max} component could be due to, for example, measurement noise, modeling error, or other regulatory mechanisms. Finally, the unknown model order, $p, q, r, s, m,$ and $n,$ limit the number of parameters.

The mathematical analysis process, thus, amounts to measuring spontaneous beat-to-beat fluctuations in $E_{\text{max}}, \text{HR}, \text{ABP},$ and CVP and then estimating the ARX parameters from these fluctuations by minimizing the residual error magnitude. Note that beat-to-beat fluctuations in E_{max} can be measured from LVP and left ventricular volume (LVV), with the aid of transient vena cava balloon occlusion to determine the LV unstressed volume (V_0), as described in detail elsewhere (6, 26) and briefly below.

It is important to note that this model does not provide a complete depiction of the dynamic relationship among the fluctuations in CVP, ABP, HR, and E_{max} . In particular, the model is open-loop and specifically represents only the feed-back pathway. Any influence of E_{max} fluctuations on CVP, ABP, and HR fluctuations is attributed to the unmodeled feed-forward pathway. See the DISCUSSION for additional model limitations.

Fig. 1. Block diagram indicating the complex relationship between beat-to-beat fluctuations in maximal ventricular elastance (E_{max}), central venous pressure (CVP), arterial blood pressure (ABP), and heart rate (HR). The dark lines and font indicate the open-loop systems sought for identification from spontaneous beat-to-beat hemodynamic variability. The gray lines and fonts show the feed-back pathway.



Data Collection

Six healthy adult mongrel dogs (20–25 kg) were studied. This study was approved by the Wayne State University Animal Investigation Committee and conformed to the National Institutes of Health guidelines. The materials and procedures are described in detail elsewhere (28), and the relevant aspects of the data collection for this particular study are briefly described as follows. Chronic instrumentation was installed in each dog through two recovery surgeries. The instrumentation included an implanted, high-fidelity pressure transducer (Data Sciences International) for LVP measurement; two pairs of sonomicrometry crystals (Sonometrics) for LV short- and long-axis dimensions (DSA and DLA) measurement and subsequent computation of LVV via the modified ellipsoid formula $(\pi/6) \times \text{DSA} \times \text{DSA} \times \text{DLA}$; two hydraulic vascular occluders (In Vivo Metrics) for superior and inferior vena cava occlusion; an ultrasonic flow probe (Transonic Systems) around the ascending aorta for aortic flow rate measurement; and two fluid-filled catheters connected to standard extracorporeal pressure transducers (Abbott Laboratories) for ABP and CVP measurements. After full recovery from the surgeries, the hemodynamic data were continuously recorded at a sampling frequency of about 300 Hz during a baseline period of 5–8 min and multiple transient vena cava occlusions, while the dog stood quietly. Propranolol was, thereafter, infused to achieve complete β -adrenergic receptor blockade in five of the dogs, and the data were likewise recorded.

Detailed Data Analysis

For each beat during the baseline periods, E_{\max} was estimated as the maximum of LVP/(LVV- V_0), where V_0 was determined from the transient vena cava occlusions via the conventional method (6, 26); HR was detected from the aortic flow rate waveform (rather than an ECG waveform) and, thus, precisely indicates the pulse rate; and ABP and CVP were averaged. The four beat sequences were then converted to 1-Hz time series (6), and the mean values of the time series were removed. The power spectra of the zero-mean time series were computed using standard AR analysis.

For a fixed-model order, the ARX parameters in Eq. 1 were estimated from the time series by linear least squares minimization of $W_{E_{\max}}$ (15). The model order terms p , n , s , and m were set to 2, 5, 2, and 2, respectively, based on previous studies of the ABP $\rightarrow E_{\max}$ and HR $\rightarrow E_{\max}$ transfer functions (6, 11). Because there are no such studies of the CVP $\rightarrow E_{\max}$ transfer function, the model order terms q and r were set to 0 and selected by minimizing the minimum description length (MDL) criterion (15). The three transfer functions were then computed from the parameter estimates using Eqs. 2–4. The static gain (i.e., transfer function at zero frequency or, equivalently, the asymptotic value of the step response) was also determined for each identified transfer function, along with the overall time constant (indicative of the time it takes for the step response to reach steady state) via a robust rectangular-based method (14). This system of identification analysis was applied to stationary segments of the time series as follows. The analysis was first applied to each 3-min segment of the time series, overlapping by 30 s, for each condition (control or β -adrenergic receptor blockade) of each subject. The 4-min segment wherein the static gains of the three transfer functions varied least was selected. The analysis was then applied to this 4-min stationary segment to yield the final estimates.

The identified transfer functions were assessed in three ways. First, squared causal coherence functions were computed (19, 22). In particular, E_{\max} fluctuations were predicted from all or one of the measured CVP, ABP, and HR fluctuations using Eq. 1 with the estimated causal ARX parameters. Ratios of the power spectrum of the predicted E_{\max} fluctuations to the power spectrum of the measured E_{\max} fluctuations were then computed. These squared causal coherence functions indicate the collective or individual ability of the transfer functions to predict E_{\max} fluctuations from only the input

fluctuations per frequency. Second, the goodness-of-fit was computed as described previously (23). This quantity reflects the variance of the residual error $W_{E_{\max}}$ and, thus, indicates the collective ability of the transfer functions to predict the current E_{\max} fluctuations from the previous E_{\max} fluctuations and the input fluctuations. For both of these assessment metrics, a value of one indicates perfect predictive ability, whereas a value of 0 indicates no predictive capacity. Third, the whiteness of the residual error $W_{E_{\max}}$ was assessed via its autocorrelation function (15). If the autocorrelation function shows significant correlation at nonzero lags, then the transfer functions are biased.

One sample and paired t -tests were employed to compare the estimated quantities in various ways. A P value of less than 0.1 was considered significant.

Finally, since the three input-single output system identification analysis here was more intricate than our previous applications of system identification (6, 17), the sensitivity of the results to user-selected quantities was evaluated. First, each selected stationary segment was perturbed by advancing and delaying its start and end times by 10% of the segment duration. System identification was then applied to the perturbed 4-min segments using the same model order that was obtained from the original segment. Second, the selected model order was perturbed by increasing and decreasing each fixed model order term, one at a time, by 1. System identification was then applied to the original stationary segments using the perturbed model orders, with the model order term r selected by minimizing the MDL criterion. The static gain of the identified CVP $\rightarrow E_{\max}$ transfer function was finally assessed as a function of the segment for analysis and the model order.

RESULTS

Spontaneous Beat-to-Beat Hemodynamic Fluctuations

Table 1 shows the group average (means \pm SE) of the mean of the CVP, ABP, HR, and E_{\max} fluctuations, as well as the group average V_0 during the control and β -adrenergic receptor blockade conditions. Figure 2 illustrates the group average power spectra of these fluctuations, while Table 1 also indicates the square root of their total powers (i.e., standard deviations). (The confidence intervals in Fig. 2 and subsequent figures were computed as the group average plus or minus the group SE and, thus, indicate the variation among subjects.) The

Table 1. Group average mean and SD of the hemodynamic variables during the control and β -adrenergic receptor blockade conditions

Hemodynamic Variable	Control	β -Adrenergic Receptor Blockade	P Value
CVP			
mean, mmHg	1.0 \pm 1.2	1.7 \pm 1.2	0.53
SD, mmHg	1.4 \pm 0.4	1.3 \pm 0.6	0.82
ABP			
mean, mmHg	98.2 \pm 4.6	96.5 \pm 6.4	0.75
SD, mmHg	4.1 \pm 0.4	3.7 \pm 0.6	0.49
HR			
mean, beats/min	98.2 \pm 7.5	87.8 \pm 6.6	0.06
SD, beats/min	11.1 \pm 1.7	7.6 \pm 1.4	0.05
E_{\max}			
mean, mmHg/ml	5.1 \pm 0.7	3.6 \pm 0.3	0.02
SD, mmHg/ml	0.23 \pm 0.07	0.09 \pm 0.02	0.10
V_0 , ml	25.1 \pm 3.7	25.1 \pm 3.4	0.12

Values are expressed as means \pm SE. CVP, central venous pressure; ABP, arterial blood pressure; HR, heart rate; E_{\max} , maximal left ventricular elastance; V_0 , left ventricular unstressed volume. HR was computed from an aortic flow rate waveform rather than an ECG waveform and, thus, precisely indicates the pulse rate.

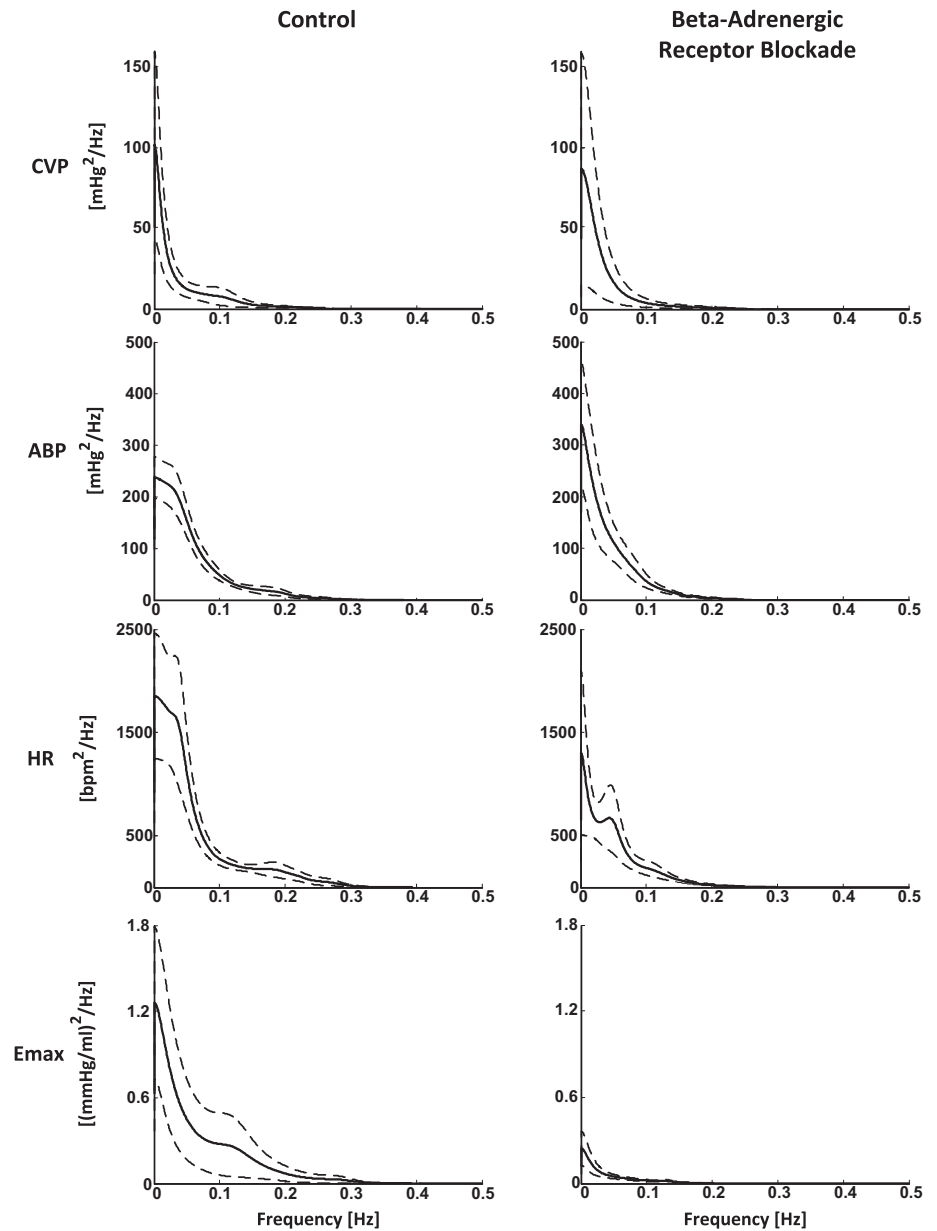


Fig. 2. Group average power spectra (means \pm SE) of the spontaneous beat-to-beat fluctuations in CVP, ABP, HR, and E_{\max} during the control and β -adrenergic receptor blockade conditions. HR variations here were computed from an aortic flow rate waveform rather than an ECG waveform and thus precisely indicate changes in the pulse rate. The confidence intervals here and in other figures were computed as the group average plus or minus the group SE and thus indicate the variation among subjects.

mean and standard deviation of the HR and E_{\max} fluctuations appreciably decreased following the beta blockade at significance levels of $P < 0.05$ or 0.10. Note that the HR fluctuations here were derived from an aortic flow rate waveform and, thus, precisely reflect variations in the pulse rate. None of the remaining quantities showed important changes. The maximal frequency of the fluctuations was no more than 0.3 Hz.

Identified Transfer Functions

Figures 3 and 4 illustrate the group average of the $CVP \rightarrow E_{\max}$, $ABP \rightarrow E_{\max}$, and $HR \rightarrow E_{\max}$ transfer functions in terms of magnitude and phase responses, as well as step responses during the control and β -adrenergic receptor blockade conditions. Table 2 shows the static gains and overall time constants of these transfer functions.

Control $CVP \rightarrow E_{\max}$. During the control condition, the $CVP \rightarrow E_{\max}$ transfer function exhibited a static gain of $0.037 \pm$

0.010 ml^{-1} (means \pm SE). This value was different from zero at a significance level of $P < 0.05$. Hence, E_{\max} would increase in the steady state in response to a step increase in CVP as a result of the cardiopulmonary baroreflex independent of any change in ABP or HR. For an average increase in CVP (i.e., standard deviation of the time series), the magnitude of the E_{\max} increase would be $0.04 \pm 0.01 \text{ mmHg/ml}$. Further, the transfer function showed bandpass-like characteristics. Hence, E_{\max} would reach steady state with some oscillations in response to a step change in CVP, with an overall time constant of $3.2 \pm 1.2 \text{ s}$.

Control $ABP \rightarrow E_{\max}$ and $HR \rightarrow E_{\max}$. During the same condition, the $ABP \rightarrow E_{\max}$ and $HR \rightarrow E_{\max}$ transfer functions exhibited static gains of $-0.012 \pm 0.003 \text{ ml}^{-1}$ and $0.014 \pm 0.002 \text{ mmHg/ml-bpm}$, respectively. These values were also different from zero at a significance level of $P < 0.05$. Hence, E_{\max} would decrease in the steady state in response to a step

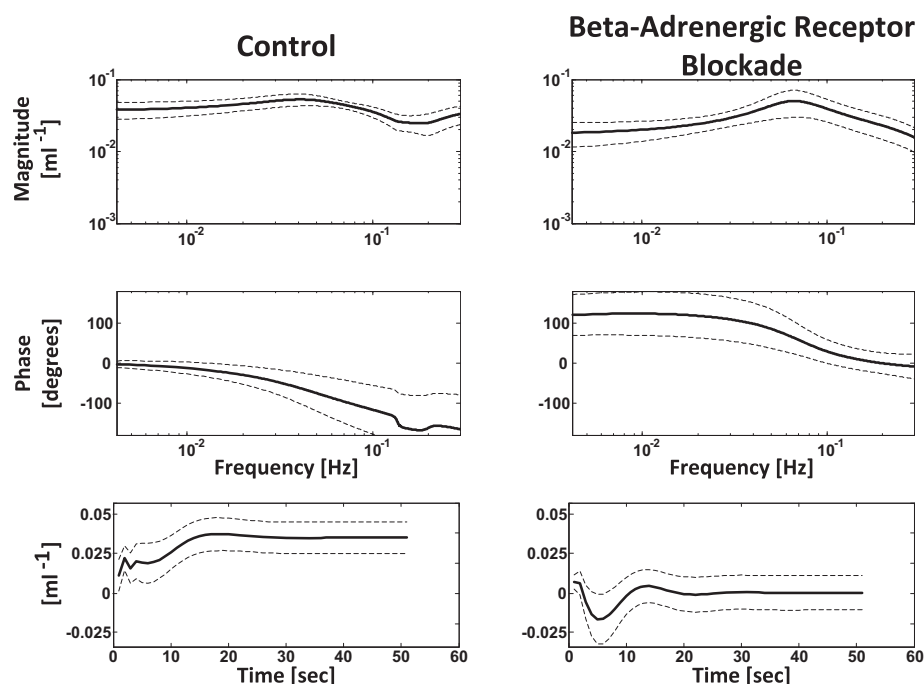
CVP \rightarrow E_{\max} 

Fig. 3. Group average CVP \rightarrow E_{\max} transfer functions in terms of magnitude and phase responses, as well as step responses (means \pm SE) during the control and β -adrenergic receptor blockade conditions.

increase in ABP due to the arterial baroreflex independent of any change in HR or CVP, whereas E_{\max} would increase in the steady state in response to a step increase in HR as a result of the force-frequency relation independent of any change in ABP or CVP. For average increases in ABP and HR, the magnitude of the E_{\max} change would be 0.05 ± 0.01 and 0.15 ± 0.03 mmHg/ml, respectively. The latter value was different from the corresponding magnitude of E_{\max} change via the cardiopulmonary baroreflex at a significance level of $P < 0.05$. So, the cardiopulmonary baroreflex contributed to about the same extent in steady-state E_{\max} control as the arterial baroreflex, but less than the force-frequency relation. Further, the ABP \rightarrow E_{\max} transfer function showed low-pass characteristics, whereas the HR \rightarrow E_{\max} transfer function showed all-pass-like characteristics with nonlinear phase response. Hence, E_{\max} would monotonically reach steady state in response to a step change in ABP or HR, with overall time constants of 7.0 ± 1.1 and 1.5 ± 0.3 s, respectively. The former value was different from the overall time constant of the cardiopulmonary baroreflex at a significance level of $P < 0.10$. So, the cardiopulmonary baroreflex was faster than the arterial baroreflex in modulating E_{\max} but not different in speed from the force-frequency relation.

β -adrenergic receptor blockade. Following the beta blockade, all three transfer functions were markedly blunted in the low-frequency regime (<0.05 Hz). The static gains were, in particular, nearly abolished at significance levels of $P < 0.05$ or 0.10 . Hence, E_{\max} would hardly change in steady state in response to a step increase in CVP, ABP, or HR. However, in the higher frequency range (>0.05 Hz), the CVP \rightarrow E_{\max} and HR \rightarrow E_{\max} transfer functions were not suppressed and perhaps even amplified after the blockade. Hence, E_{\max} would transiently change to some extent in response to a step increase in CVP or HR, but not ABP. So, like the arterial baroreflex and

force-frequency relation, the cardiopulmonary baroreflex controlled E_{\max} via β -adrenergic receptor system mediation.

Transfer Function Assessment

Squared causal coherence. Figure 5 illustrates the group average of the squared causal coherence functions for all three transfer functions during the control and β -adrenergic receptor blockade conditions. The average squared causal coherence over frequency was 0.56 ± 0.10 during the control condition and 0.48 ± 0.12 following the β -blockade. Hence, the cardiopulmonary baroreflex, arterial baroreflex, and force-frequency relation collectively accounted for about 70% of the standard deviation of the entire E_{\max} fluctuations (i.e., square root of coherence) during both conditions.

During the control condition, the average squared causal coherence over frequency was 0.08 ± 0.02 for the CVP \rightarrow E_{\max} transfer function, 0.03 ± 0.01 for the ABP \rightarrow E_{\max} transfer function, and 0.46 ± 0.09 for the HR \rightarrow E_{\max} transfer function. (Consistent with the overall squared causal coherence function of Fig. 5, the average coherence functions for each transfer function showed a peak at 0.04 Hz, while the coherence function for the HR \rightarrow E_{\max} transfer function also showed a peak at 0.25 Hz.) The value for the HR \rightarrow E_{\max} transfer function was different from that of the CVP \rightarrow E_{\max} transfer function at a significance level of $P < 0.05$. Hence, during the control condition, the cardiopulmonary baroreflex accounted for about 40% as much of the standard deviation of the E_{\max} fluctuations as the force-frequency relation but contributed similarly to dynamic E_{\max} control as the arterial baroreflex. Following the β -adrenergic receptor blockade, the corresponding coherence was 0.24 ± 0.09 for the CVP \rightarrow E_{\max} transfer function, 0.014 ± 0.005 for the ABP \rightarrow E_{\max} transfer function, and 0.31 ± 0.1 for the HR \rightarrow E_{\max} transfer function. The value

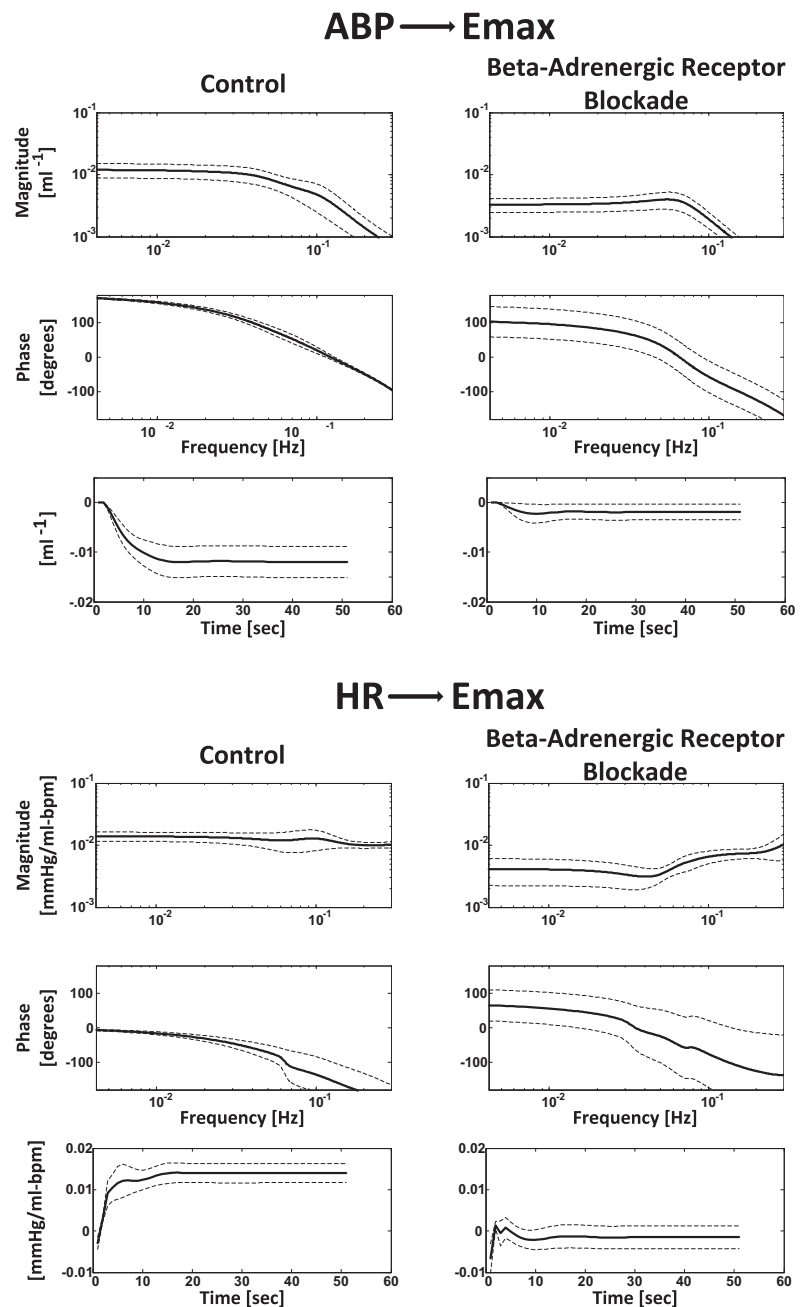


Fig. 4. Group average $ABP \rightarrow E_{\max}$ and $HR \rightarrow E_{\max}$ transfer functions in terms of magnitude and phase responses, as well as step responses (means \pm SE) during the control and β -adrenergic receptor blockade conditions.

for the $ABP \rightarrow E_{\max}$ transfer function was different from the other transfer functions at a significance level of $P < 0.05$ or $P < 0.10$. So, after β -adrenergic receptor blockade, the cardiopulmonary baroreflex contributed similarly to dynamic E_{\max} control as the force-frequency relation but more than the arterial baroreflex.

Goodness-of-fit. The group average of the goodness-of-fit was 0.95 ± 0.02 during the control condition and 0.93 ± 0.02 following β -adrenergic receptor blockade. Hence, the cardiopulmonary baroreflex, arterial baroreflex, and force-frequency relation accounted for most of the present E_{\max} fluctuations during both conditions.

Residual whiteness. The autocorrelation functions of the residual error for each condition of each subject generally showed nonzero amplitudes for lags of 1 and 2 s at a signifi-

cance level of $P < 0.05$. So, the residual error was not white, and the transfer functions were biased. However, because of the short-ranging residual error correlation, the bias may not have adversely impacted the transfer functions at lower frequencies, especially the static gains.

Sensitivity analysis. Figure 6 shows the static gain of the $CVP \rightarrow E_{\max}$ transfer function from the control condition as a function of perturbations to the data segments chosen for analysis and the selected model order. The static gains were not very sensitive to the perturbations. These sensitivity analysis results support the major finding that the cardiopulmonary baroreflex responds to an increase in CVP by increasing E_{\max} with a static gain of around 0.037 ml^{-1} . Note that altering the model order term p in Eq. 1 changes the number of time constants of the system. Reducing p from 2 to 1 had great

Table 2. Group average static gains and overall time constants of the transfer functions relating beat-to-beat fluctuations in CVP to E_{max} ($CVP \rightarrow E_{max}$), ABP to E_{max} ($ABP \rightarrow E_{max}$), and HR to E_{max} ($HR \rightarrow E_{max}$) during the control and β -adrenergic receptor blockade conditions

Transfer Function Quantity	Control	β -Adrenergic Receptor Blockade	P Value
Static Gain			
CVP $\rightarrow E_{max}$, ml $^{-1}$	0.037 \pm 0.010 ($P = 0.016$)	0.0007 \pm 0.0113	$P = 0.081$
ABP $\rightarrow E_{max}$, ml $^{-1}$	-0.012 \pm 0.003 ($P = 0.013$)	-0.0019 \pm 0.0016	$P = 0.079$
HR $\rightarrow E_{max}$, mmHg/ml-bpm	0.014 \pm 0.002 ($P = 0.002$)	-0.0015 \pm 0.003	$P = 0.031$
Overall Time Constant			
CVP $\rightarrow E_{max}$, s	3.2 \pm 1.2	*	NA
ABP $\rightarrow E_{max}$, s	7.0 \pm 1.1	*	NA
HR $\rightarrow E_{max}$, s	1.5 \pm 0.3	*	NA
	($P = 0.003$)	[($P = 0.088$)] ($P = 0.23$)

Values are expressed as means \pm SE. *Overall time constants were not well defined because of the relatively small transfer function magnitudes. The P values in parentheses reflect the results of one-sample t -tests comparing the mean to 0.

impact on the static gain simply because one time constant was insufficient to capture the system dynamics. For this reason, perturbations to the term p were not included in these sensitivity analysis results.

DISCUSSION

The cardiopulmonary baroreflex responds to an increase in CVP by decreasing TPR and increasing HR in dogs (3, 17, 25). However, the direction of ventricular contractility change, if any, is not well understood. To elucidate the cardiopulmonary baroreflex control of ventricular contractility, a reliable ventricular contractility index should be obtained, while eliminating confounding physiological mechanisms.

One potential approach is experimental. For example, sinoaortic denervation and fixed-rate cardiac pacing could be performed to abolish the arterial baroreflex and force-frequency relation. Average E_{max} , which is perhaps the best available index of ventricular contractility, could then be determined from LVP and LVV measurements during transient vena cava occlusion at different average CVP levels induced by total blood volume changes. A simple plot of E_{max} vs. CVP would reveal the direction, as well as magnitude of the ventricular contractility change.

An alternative approach is mathematical. We chose to take this approach. More specifically, we measured spontaneous beat-to-beat fluctuations in E_{max} , CVP, ABP, and HR from awake dogs before and after β -adrenergic receptor blockade. We then employed an ARX model to jointly identify the causal CVP $\rightarrow E_{max}$, ABP $\rightarrow E_{max}$, and HR $\rightarrow E_{max}$ transfer functions

from the measured fluctuations. By performing this three input-single output system identification, the resulting CVP $\rightarrow E_{max}$ transfer function indicated the E_{max} response to a fixed change in CVP, while ABP and HR are held constant, due to the cardiopulmonary baroreflex. In this way, the arterial baroreflex and force-frequency relation were mathematically eliminated. While similar mathematical analyses have been previously applied to elucidate causal, dynamic relationships between beat-to-beat hemodynamic fluctuations (2, 4, 6, 8, 13, 18, 19, 22, 32), only a few were employed to investigate the cardiopulmonary baroreflex (17, 20).

There are two major advantages of our mathematical analysis study over the experimental study. First, the CVP $\rightarrow E_{max}$ transfer function does not just indicate the direction and magnitude of the change in ventricular contractility (static behavior) but also how quickly the system makes the change (dynamic behavior). Second, these behaviors are ascertained during normal physiological conditions rather than experimental interventions, such as sinoaortic denervation, which typically alter the functionality of the cardiopulmonary baroreflex (17, 25).

On the other hand, the disadvantage of any mathematical analysis study is the assumptions upon which it is based. There are two major assumptions underlying our mathematical analysis. First, the control of ventricular contractility is linear and time-invariant. While this assumption is generally incorrect, it may be approximately true for the small, resting fluctuations that were studied here (32). The average squared causal coherences of near or above 0.5 and the goodness-of-fits exceeding 0.9 that we obtained support this assumption (11, 23). However, the identified transfer functions are only representative of the system dynamics over the limited range of the measured spontaneous hemodynamic variability. If the range of variability were to change, then the transfer functions should be reidentified. Second, the information present in the spontaneous fluctuations is sufficient to simultaneously identify three systems. To make this assumption more tenable, we employed an ARX model and limited the number of parameters to identify these systems. (Note that the chosen value for the model order term r in Eq. 1 was typically 2 or 3.) This succinct representation, especially the low AR order of 2, was not sufficient to whiten the residual error ($W_{E_{max}}$ in Eq. 1). Hence, the identified transfer functions were not unbiased and, therefore, have a clear limitation. However, the residual error correlation was short ranging, so the bias may not have impacted the static gains. The static gain of the CVP $\rightarrow E_{max}$

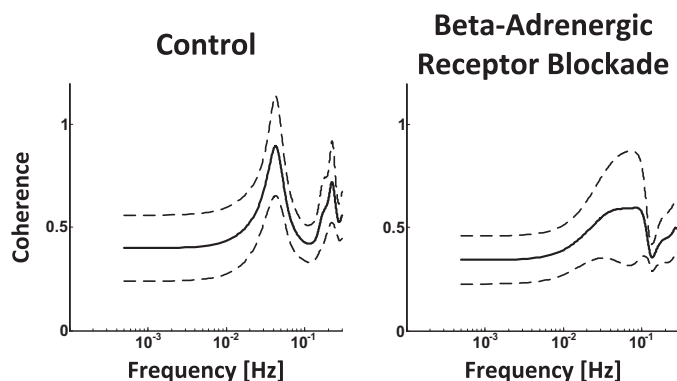


Fig. 5. Group average squared causal coherence functions (means \pm SE) for all three transfer functions during the control and β -adrenergic receptor blockade conditions.

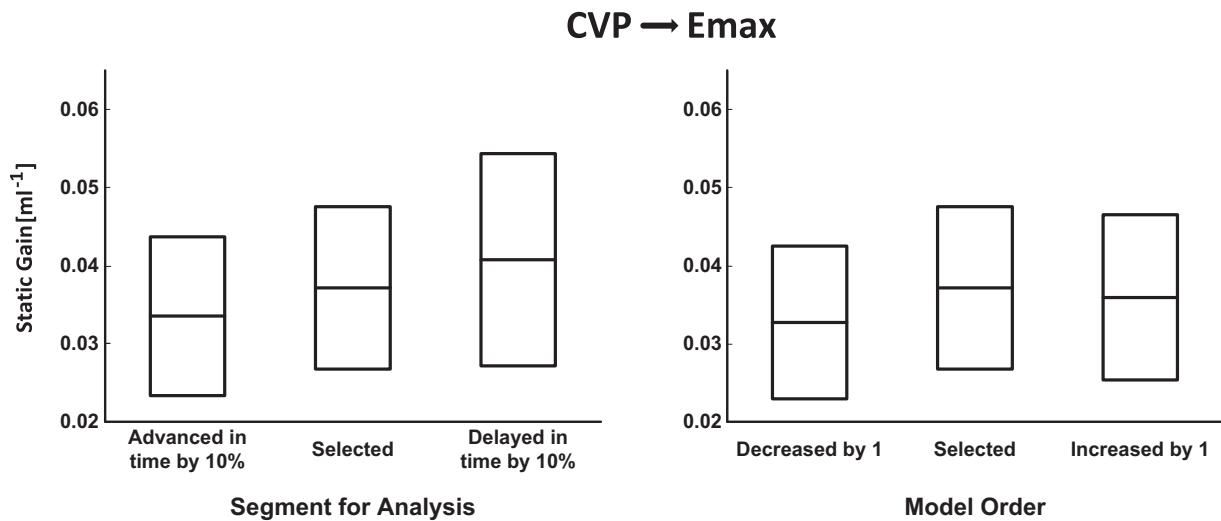


Fig. 6. Group average static gain of the CVP → E_{\max} transfer function (means ± SE) as a function of perturbations to the data segment chosen for analysis (left) and the selected model order (right). The static gains for the perturbed model orders represent the average of individual perturbations to n , s , m , and q in Eq. 1.

transfer function, in particular, constitutes the major finding of this study. By accepting some bias, the precision of the identified transfer functions was reduced to a greater extent. Further, we performed a sensitivity analysis to determine how robust the static gain of the CVP → E_{\max} transfer function was to perturbations to the user-selected quantities of the mathematical analysis.

The principal results of our mathematical analysis study are as follows. First, the cardiopulmonary baroreflex responds to an increase in CVP by increasing E_{\max} (static gain of $0.037 \pm 0.010 \text{ ml}^{-1}$). Second, the cardiopulmonary baroreflex contributes to about the same extent in modulating E_{\max} as the arterial baroreflex, but less than the force-frequency relation (change in the magnitude of E_{\max} of 0.04 mmHg/ml for an average change in CVP). Third, the cardiopulmonary baroreflex is faster than the arterial baroreflex in controlling E_{\max} but not different in speed from the force-frequency relation (overall time constant of $3.2 \pm 1.2 \text{ s}$). Fourth, the cardiopulmonary baroreflex hardly changes E_{\max} in steady state in response to an increase in CVP following β -adrenergic receptor blockade (static gain of 0.0007 ± 0.0113). So, stimulation of the cardiopulmonary baroreflex appreciably increases ventricular contractility, reaching a maximal level in about 16 s, through changes in cardiac sympathetic nerve activity.

Importantly, the cardiopulmonary baroreflex control of E_{\max} was not fast, with a high-cutoff frequency within 0.1 Hz. This frequency is less than the typical respiratory rate of dogs. Hence, using CVP minus intrathoracic pressure (i.e., transmural pressure) as the system input or including respiration as a fourth input may not have significantly impacted the results. However, we acknowledge the possibility that respiratory activity, which was not measured, could have been irregular here, such that its exclusion would constitute a clear study limitation.

Ancillary results of this study include the following. The arterial baroreflex responds to an increase in ABP by decreasing E_{\max} (static gain of $-0.012 \pm 0.003 \text{ ml}^{-1}$), while the force-frequency relation responds to an increase in HR by increasing E_{\max} (static gain of $0.014 \pm 0.002 \text{ mmHg/ml-bpm}$). Further, as indicated in the above paragraph, the arterial baro-

reflex is more sluggish in modulating E_{\max} than the force-frequency relation. Finally, both of these systems have little impact on E_{\max} after β -adrenergic receptor blockade (static gains of $-0.0019 \pm 0.0016 \text{ ml}$ and $-0.0015 \pm 0.0030 \text{ mmHg/ml-bpm}$). These secondary results are consistent with known physiology. If such consistency were not obtained, then the new results on the cardiopulmonary baroreflex from this study would have been in serious doubt.

As further confirmation, the sensitivity analysis indicated that the static gain of the CVP → E_{\max} transfer function was not highly sensitive to the data segments chosen for analysis and the selected model order. This result specifically buttresses the key finding that the cardiopulmonary baroreflex responds to an increase in CVP by increasing E_{\max} with a static gain in the range of 0.037 ml^{-1} . We also performed a further sensitivity analysis to assess the robustness of the results to wide perturbations to the model order. More specifically, we selected more than 30,000 candidate model orders that were within double of the originally selected model order. We then identified the three transfer functions for each of these model orders. The model orders that yielded nonphysiological results for the ABP → E_{\max} transfer function (i.e., positive static gain) and/or the HR → E_{\max} transfer function (i.e., negative static gain) were discarded, since the results for the CVP → E_{\max} transfer function would likely be nonphysiological as a result of the interdependencies of the three jointly identified systems. The CVP → E_{\max} transfer function identified with the remaining model orders (>10,000) were assessed. The static gain was positive 91% of the time. This additional result helps confirm the most important finding that stimulation of the cardiopulmonary baroreflex increases ventricular contractility. Note that we could not similarly perform a sensitivity analysis to further assess the robustness to the segments for analysis due to the limited duration of the available data.

The key finding of our mathematical analysis study is consistent with the experimental studies of Karim et al. (10) and Kurz et al. (12), in which cardiac sympathetic nerve activity and the maximal LVP derivative (with some preload compensation) increased with left atrial balloon distension in

anesthetized dogs. However, our result conflicts with the experimental study of Ramchandra et al. (24), in which cardiac sympathetic nerve activity decreased with increasing CVP during blood volume changes in conscious sheep. The opposing result may be due to the presence of confounding physiological mechanisms (e.g., arterial baroreflex) in their study and possibly species differences. Our finding also contrasts with the experimental study of Furnival et al. (9), in which the maximal LVP derivative did not change with left atrial balloon distension in anesthetized dogs. Other than the use of different ventricular contractility indices, it is difficult to come up with a reason explaining their result with our finding and the results of Karim et al. (10) and especially Kurz et al. (12).

Our study is also closely related to the mathematical analysis study of Chen et al. (6), in which the $ABP \rightarrow E_{\max}$ and $HR \rightarrow E_{\max}$ transfer functions were identified from spontaneous ABP, HR, and E_{\max} fluctuations in awake dogs without consideration for the cardiopulmonary baroreflex. It is, thus, interesting to determine how inclusion of CVP fluctuations as a third input impacts the $ABP \rightarrow E_{\max}$ and $HR \rightarrow E_{\max}$ transfer functions. So, we identified these transfer functions without using CVP fluctuations from the same experimental subjects during the control condition. The static gain and overall time constant for the $HR \rightarrow E_{\max}$ transfer function were 0.010 ± 0.002 mmHg/ml-bpm and 1.2 ± 0.2 s without CVP inclusion and 0.014 ± 0.002 mmHg/ml-bpm and 1.5 ± 0.03 s with CVP inclusion, while the static gain and overall time constant for the $ABP \rightarrow E_{\max}$ transfer function were -0.036 ± 0.014 ml⁻¹ and 11.2 ± 3.1 s without CVP inclusion and -0.012 ± 0.03 ml⁻¹ and 7 ± 1.1 s with CVP inclusion. The $HR \rightarrow E_{\max}$ static gains were different at a significance level of $P < 0.10$. Further, the average squared causal coherence over frequency for all transfer functions was 0.47 ± 0.01 without CVP inclusion and 0.56 ± 0.10 with CVP inclusion. Hence, inclusion of CVP fluctuations in the mathematical analysis had some quantitative, but not directional, impact on the $ABP \rightarrow E_{\max}$ and $HR \rightarrow E_{\max}$ transfer functions and yields some improvement in the prediction of the E_{\max} fluctuations.

Perspectives and Significance

In summary, stimulation of the cardiopulmonary baroreflex increases ventricular contractility in awake dogs so as to maintain CVP, much like the Bainbridge effect. The contribution of the cardiopulmonary baroreflex to ventricular contractility control during normal physiological conditions is similar to the arterial baroreflex. Hence, cardiopulmonary baroreflex control of ventricular contractility plays a significant role in blood pressure regulation. This mechanism is blunted by β -adrenergic receptor blockade. How this regulation is altered in situations of increased baseline sympathetic tone (e.g., exercise, β -adrenergic agonists), as well as in pathophysiological states (heart failure/hypertension/diabetes, etc.), is unknown. Finally, to what extent these relationships might vary in humans is unclear and worthy of future investigation.

GRANTS

This work was supported by the National Institutes of Health (HL-55473, HL-095819, HL-080568), the National Science Foundation (CAREER 0643477), and by the Telemedicine and Advanced Technology Research Center (TATRC) at the U.S. Army Medical Research and Materiel Command (USAMRMC) through award W81XWH-10-2-0124.

DISCLOSURES

No conflicts of interest, financial or otherwise, are declared by the authors.

AUTHOR CONTRIBUTIONS

Author contributions: J.A.S.-M., R.L.H., M.I., and S.E. performed experiments; J.A.S.-M., M.M., R.L.H., M.I., X.C., S.E., D.S.O., and R.M. approved final version of manuscript; M.M. and X.C. analyzed data; M.M. and R.M. interpreted results of experiments; M.M. prepared figures; M.M. and R.M. drafted manuscript; R.L.H. and D.S.O. edited and revised manuscript; R.M. conception and design of research.

REFERENCES

1. Abboud FM, Eckberg DL, Johannsen UJ, Mark AL. Carotid and cardiopulmonary baroreceptor control of splanchnic and forearm vascular resistance during venous pooling in man. *J Physiol* 286: 173–184, 1979.
2. Appel ML, Berger RD, Saul JP, Smith JM, Cohen RJ. Beat to beat variability in cardiovascular variables: Noise or music? *J Am Coll Cardiol* 14: 1139–1148, 1989.
3. Bainbridge FA. The influence of venous filling upon the rate of the heart. *J Physiol* 50: 65–84, 1915.
4. Baselli G, Cerutti S, Civardi S, Malliani A, Pagani M. Cardiovascular variability signals: towards the identification of a closed-loop model of the neural control mechanisms. *IEEE Trans Biomed Eng* 35: 1033–1046, 1988.
5. Bishop VS, Malliani A, Thorén P. Cardiac mechanoreceptors. In: *Handbook of Physiology. The Cardiovascular System. Peripheral Circulation and Organ Blood Flow*. Bethesda, MD: Am. Physiol. Soc., 1983, sect. 2, vol. III, pt. 2, chapt. 15, p. 497–555.
6. Chen X, Sala-Mercado a J, Hammond RL, Ichinose M, Soltani S, Mukkamala R, O'Leary DS. Dynamic control of maximal ventricular elastance via the baroreflex and force-frequency relation in awake dogs before and after pacing-induced heart failure. *Am J Physiol Heart Circ Physiol* 299: H62–H69, 2010.
7. Desai TH, Collins JC, Snell M, Mosqueda-Garcia R. Modeling of arterial and cardiopulmonary baroreflex control of heart rate. *Am J Physiol Heart Circ Physiol* 272: H2343–H2352, 1997.
8. Faes L, Porta A, Cucino R, Cerutti S, Antolini R, Nollo G. Causal transfer function analysis to describe closed loop interactions between cardiovascular and cardiorespiratory variability signals. *Biol Cybern* 90: 390–399, 2004.
9. Furnival CM, Linden RJ, Snow HM. Reflex effects on the heart of stimulating left atrial receptors. *J Physiol* 218: 447–463, 1971.
10. Karim F, Kidd C, Malpus CM, Penna PE. The effects of stimulation of the left atrial receptors on sympathetic efferent nerve activity. *J Physiol* 227: 243–260, 1972.
11. Kubota T, Alexander J, Itaya R, Todaka K, Sugimachi M, Sunagawa K, Nose Y, Takeshita A. Dynamic effects of carotid sinus baroreflex on ventricular-arterial coupling studied in anesthetized dogs. *Circ Res* 70: 1044–1053, 1992.
12. Kurz MA, Wead WB, Roberts AM. Reflex inotropic responses to distension of left atrium or pulmonary veins. *Am J Physiol Heart Circ Physiol* 258: H121–H126, 1990.
13. Lanfranchi PA, Somers VK. Arterial baroreflex function and cardiovascular variability: interactions and implications. *Am J Physiol Regul Integr Comp Physiol* 283: R815–R826, 2002.
14. Lathi BP. *Linear Systems and Signals (Oxford Series in Electrical and Computer Engineering)*. New York, NY: Oxford University Press, 2004.
15. Ljung L. *System Identification: Theory for the User*. 2nd ed. Englewood Cliffs, NJ: Prentice Hall, 1999.
16. Lloyd TC, Fried JJ. Effect of a left atrium-pulmonary vein baroreflex on peripheral vascular beds. *Am J Physiol Heart Circ Physiol* 233: H587–H591, 1977.
17. Mukkamala R, Kim JK, Li Y, Sala-Mercado J, Hammond RL, Scislo TJ, O'Leary DS. Estimation of arterial and cardiopulmonary total peripheral resistance baroreflex gain values: validation by chronic arterial baroreceptor denervation. *Am J Physiol Heart Circ Physiol* 290: H1830–H1836, 2006.
18. Mullen TJ, Appel ML, Mukkamala R, Mathias JM, Cohen RJ. System identification of closed-loop cardiovascular control: effects of posture and autonomic blockade. *Am J Physiol Heart Circ Physiol* 272: H448–H461, 1997.
19. Nollo G, Faes L, Porta A, Antolini R, Ravelli F. Exploring directionality in spontaneous heart period and systolic pressure variability interactions in

- humans: implications in the evaluation of baroreflex gain. *Am J Physiol Heart Circ Physiol* 288: H1777–H1785, 2005.
20. **O’Leary DD, Shoemaker JK, Edwards MR, Hughson RL.** Spontaneous beat-by-beat fluctuations of total peripheral and cerebrovascular resistance in response to tilt. *Am J Physiol Regul Integr Comp Physiol* 287: R670–R679, 2004.
 21. **Oren RM, Schobel HP, Weiss RM, Stanford W, Ferguson DW.** Importance of left atrial baroreceptors in the cardiopulmonary baroreflex of normal humans. *J Appl Physiol* 74: 2672–2680, 1993.
 22. **Porta A, Furlan R, Rimoldi O, Pagani M, Malliani A, van de Borne P.** Quantifying the strength of the linear causal coupling in closed loop interacting cardiovascular variability signals. *Biol Cybern* 86: 241–251, 2002.
 23. **Porta A, Tobaldini E, Gnecci-Ruscone T, Montano N.** RT variability unrelated to heart period and respiration progressively increases during graded head-up tilt. *Am J Physiol Heart Circ Physiol* 298: H1406–H1414, 2010.
 24. **Ramchandra R, Hood SG, Watson AMD, May CN.** Responses of cardiac sympathetic nerve activity to changes in circulating volume differ in normal and heart failure sheep. *Am J Physiol Regul Integr Comp Physiol* 295: R719–R726, 2008.
 25. **Raymundo H, Scher AM, O’Leary DS, Sampson PD.** Cardiovascular control by arterial and cardiopulmonary baroreceptors in awake dogs with atrioventricular block. *Am J Physiol Heart Circ Physiol* 257: H2048–H2058, 1989.
 26. **Sagawa K, Suga H, Shoukas AA, Bakalar KM.** End-systolic pressure/volume ratio: a new index of ventricular contractility. *Am J Cardiol* 40: 748–753, 1977.
 27. **Sala-Mercado a J, Chen X, Hammond RL, Ichinose M, O’Leary DS, Mukkamala R.** Pilot canine investigation of the cardiopulmonary baroreflex control of ventricular contractility. *Conf Proc IEEE Eng Med Biol Soc* 2009: 1852–1855, 2009.
 28. **Sala-Mercado JA, Hammond RL, Kim JK, McDonald PJ, Stephenson LW, O’Leary DS.** Heart failure attenuates muscle metaboreflex control of ventricular contractility during dynamic exercise. *Am J Physiol Heart Circ Physiol* 292: H2159–H2166, 2007.
 29. **Thrasher TN.** Unloading arterial baroreceptors causes neurogenic hypertension. *Am J Physiol Regul Integr Comp Physiol* 282: R1044–R1053, 2002.
 30. **Thrasher TN.** Effects of chronic baroreceptor unloading on blood pressure in the dog. *Am J Physiol Regul Integr Comp Physiol* 288: R863–R871, 2005.
 31. **Wellstead PE, Edmunds JM.** Least-squares identification of closed-loop systems. *Int J Control* 21: 689–699, 1975.
 32. **Xiao X, Mullen TJ, Mukkamala R.** System identification: a multi-signal approach for probing neural cardiovascular regulation. *Physiol Meas* 26: R41–R71, 2005.

